

6. Mechaber, W. L. & Hildebrand, J. G. Novel non-solanaceous host plant record for *Manduca sexta* (Lepidoptera: Sphingidae) in the southwestern United States. *Ann. Entomol. Soc. Am.* **93**, 447–451 (2000).
7. Bell, R. A., Owens, C. D., Shapiro, M. & Tardif, J. R. in *The Gypsy Moth: Research Toward Integrated Pest Management*. (eds Doane, C. C. & McManus, M. L.) 599–633 (USDA-FS Technical Bulletin 1584 (Washington DC, 1981).
8. Croasmun, W. A. & Carlson, R. M. K. (eds) *Two-Dimensional NMR spectroscopy. Applications for Chemists and Biochemists* 2nd edn (VCH, New York, 1994).
9. Yajara, S. et al. Steroidal glycosides, indiosides A–E, from *Solanum indicum*. *Phytochemistry* **43**, 1319–1323 (1996).
10. Dethier, V. G. & Crnjar, R. M. Candidate codes in the gustatory system of caterpillars. *J. Gen. Physiol.* **79**, 549–569 (1982).
11. Bernays, E. A. Selective attention and host-plant specialization. *Entomol. Exp. Appl.* **80**, 125–131 (1996).
12. Waldbauer, G. P. & Fraenkel, G. Feeding on normally rejected plants by maxillectomized larvae of the tobacco hornworm, *Protoparce sexta* (Lepidoptera, Sphingidae). *Ann. Ent. Soc. Am.* **54**, 477–485 (1961).
13. de Boer, G. Role of bilateral chemosensory input in food discrimination by *Manduca sexta*. *Entomol. Exp. Appl.* **61**, 159–168 (1991).
14. de Boer, G. Effect of diet experience on the ability of different larval chemosensory organs to mediate food discrimination by the tobacco hornworm, *Manduca sexta*. *J. Insect Physiol.* **37**, 763–769 (1991).
15. Flowers, R. W. & Yamamoto, R. T. Feeding on non-host plants by partially maxillectomized tobacco hornworms (*Manduca sexta*: Lepidoptera: Sphingidae). *Florida Entomol.* **75**, 89–93 (1992).
16. de Boer, G. Plasticity in food preference and diet-induced differential weighting of chemosensory information in larval *Manduca sexta*. *J. Insect Physiol.* **12**, 17–24 (1993).
17. Schoonhoven, L. M. & Dethier, V. G. Sensory aspects of host plant discrimination by lepidopterous larvae. *Arch. Neder. Zool.* **16**, 497–530 (1966).
18. Schoonhoven, L. M. Sensitivity changes in some insect chemoreceptors and their effect on food selection behavior. *Proc. K. Ned. Akad. Wet. C* **72**, 491–498 (1969).
19. Städler, E. & Hanson, F. E. in *Host Plant in Relation to Insect Behavior and Reproduction* (ed. Jermy, T.) 267–273 (Plenum, New York, 1976).
20. Abisgold, J. D. & Simpson, S. J. The effect of dietary protein levels and haemolymph composition on the sensitivity of maxillary palp chemoreceptors of locusts. *J. Exp. Biol.* **135**, 215–229 (1988).
21. Glendinning, J. L., Ensslen, S., Eisenberg, E. & Weiskopf, P. Diet-induced plasticity in the taste system of an insect: localization to a single transduction pathway in an identified taste cell. *J. Exp. Biol.* **202**, 2091–2102 (1999).
22. Rothschild, M., Aplin, R. & Marsh, N. Toxicity induced in the tobacco horn-worm (*Manduca sexta* L.) (Sphingidae, Lepidoptera). *Nature* **280**, 487–488 (1979).
23. Gothilf, S. E. & Hanson, F. E. Technique for electrophysiologically recording from sensory organs of intact caterpillars. *Entomol. Exp. Appl.* **72**, 305–310 (1994).

Acknowledgements

We thank J. Ewer, K. Whitlock, D. Bodnar, C. Gilbert, P. Rivlin and J. Bestman for critical reviews of the manuscript; M. Haribal for preliminary NMR and MS; B. Johnson for equipment to analyse electrophysiological recordings; and J. Almadovar and M. Chu for help in the laboratory. This work was supported by grants from the NSF and the Binational Science Foundation to R.B., and the NSF to C.I.M.

Correspondence and requests for materials should be addressed to M.L.d.C. (e-mail: moliva@binghamton.edu).

Scalable architecture in mammalian brains

Damon A. Clark*†, Partha P. Mitra‡ & Samuel S.-H. Wang*

* Department of Molecular Biology and † Department of Physics, Princeton University, Princeton, New Jersey 08544, USA

‡ Bell Laboratories, Lucent Technologies, 600 Mountain Avenue, Murray Hill, New Jersey 07974, USA

Comparison of mammalian brain parts has often focused on differences in absolute size^{1–3}, revealing only a general tendency for all parts to grow together². Attempts to find size-independent effects using body weight as a reference variable¹ obscure size relationships owing to independent variation of body size⁴ and give phylogenies of questionable significance⁵. Here we use the brain itself as a size reference to define the cerebrotyp, a species-by-species measure of brain composition. With this measure, across many mammalian taxa the cerebellum occupies a constant fraction of the total brain volume (0.13 ± 0.02), arguing against the hypothesis that the cerebellum acts as a computational engine

principally serving the neocortex³. Mammalian taxa can be well separated by cerebrotyp, thus allowing the use of quantitative neuroanatomical data to test evolutionary relationships. Primate cerebrotypes have progressively shifted and neocortical volume fractions have become successively larger in lemurs and lorises, New World monkeys, Old World monkeys, and hominoids, lending support to the idea that primate brain architecture has been driven by directed selection pressure⁴. At the same time, absolute brain size can vary over 100-fold within a taxon, while maintaining a relatively uniform cerebrotyp. Brains therefore constitute a scalable architecture.

Components of the brain make many more connections to one another than to any external structure. Furthermore, body size is under separate developmental and environmental control, rendering it an approximate reference measure at best⁴. Comparison of brain components across species, therefore, would be facilitated by a size measure that is independent of body parameters. To address this need for an internal normalization, we calculated the volume fraction (*F*) for each component, defining the total brain volume within each species as 1. We called the set of all the volume fractions for a species the cerebrotyp.

A database of insectivores and primates⁶ showed significant variation of the cerebrotyp (Fig. 1a, c). In insectivores, *F* did not vary systematically with brain size for any principal developmental brain division (Fig. 1a), therefore providing a baseline trend for comparison. By contrast, primates showed a strong trend for telencephalic growth¹. *F*_{telen} (volume fraction of telencephalon) was 60 ± 4% (mean ± s.d.; *n* = 28 species) in insectivores and 61 ± 1% in Scandentia (tree shrews; *n* = 3) but increased to 74 ± 5% in primates (*n* = 44). This increase occurred largely at the expense of medulla, mesencephalon and diencephalon: *F*_{med} + *F*_{mesen} + *F*_{dien} respectively, was 27 ± 3% in insectivores and 26 ± 1% in tree shrews, and decreased to 14 ± 4% in primates. This trade-off was emphasized by the ratio *F*_{telen}/(*F*_{med} + *F*_{mesen} + *F*_{dien}), which was 2.3 ± 0.4 in insectivores, 2.3 ± 0.2 in tree shrews, 6.3 ± 3.2 in primates and 20.8 in *Homo sapiens*.

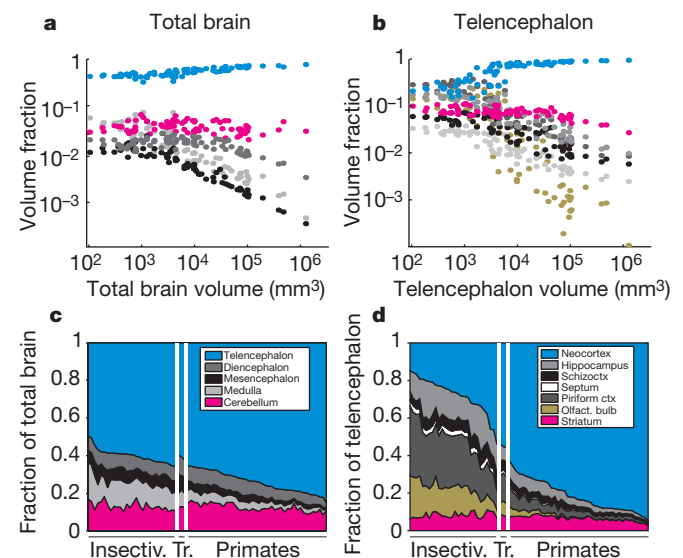


Figure 1 Analysis of volumetric data from mammalian brains. **a**, Volume fractions of principal brain divisions plotted against total brain volume. The colours are as indicated in **c**. **b**, Volume fractions of telencephalon subcomponents. The colours are as indicated in **d**. **c**, Area plot of principal brain-division volume fractions sorted by increasing telencephalic volume fraction within each taxon, demonstrating relative changes in non-cerebellar structures. Horizontal bars indicate the taxonomic groupings of insectivores (Insectiv.), tree shrews (Tr.) and primates. **d**, Area plot of telencephalic subcomponent volume fractions sorted by increasing neocortical volume fraction of the telencephalon.

Studies using body-weight-referenced scaling or comparison of absolute volumes³ suggested that cerebellum and neocortex vary together, leading to the proposition that the cerebellum is a computational engine that serves the needs of the neocortex. By contrast, we found that F_{cbl} (volume fraction of cerebellum) remained nearly constant across groups in the ref. 6 data set ($13.2 \pm 2.2\%$ in insectivores, $12.7 \pm 0.2\%$ in tree shrews and $12.4 \pm 2.1\%$ in primates; Fig. 1c, red points). To explore the generality of this finding, we examined F_{cbl} across 19 mammalian taxa (Fig. 2). F_{cbl} values across taxa remained constant ($13.5 \pm 2.4\%$) even as F_{neo} (volume fraction of neocortex) expanded from $16 \pm 6\%$ in Soricomorpha to $74 \pm 5\%$ in Hominoidea (apes and humans). Across this range of species, we found no correlation between F_{neo} and F_{cbl} ($r^2 = 0.013$, $n = 19$). The constancy of cerebellum in mammals suggests that its functional role must be evaluated not in terms of neocorticalization, but rather with either coordinated whole-brain function or some aspect of body plan that correlates strongly with total brain size.

F_{cbl} may be constrained by the high rate of energy consumption by brain tissue⁷, which would exert selection pressure for structures not to exceed a minimum essential size. Conversely, any taxon-specific increases in F_{cbl} might reflect necessary adaptations related to the addition of new functions. The cerebellum has been suggested to transform sensory information as a means of guiding motor activity. We found significantly higher values of F_{cbl} in mammals with sophisticated echolocating abilities⁸: Cetacea^{9–12} (dolphins and whales, $19 \pm 3\%$, 7 species; different from F_{cbl} in other taxa by two-tailed significance test, $P < 0.02$) and Microchiroptera¹³ (microbats, $22 \pm 5\%$, 225 species; different from other taxa, $P < 0.01$). In contrast to Microchiroptera, the Megachiroptera (megabats), which lack the ability to echolocate, did not have unusually large cerebella ($F_{\text{cbl}} = 14 \pm 1\%$, 47 species; $P = 0.97$), suggesting that adaptations to bat body plan alone were not responsible for the cerebellar enlargement. The observed size differences may be region specific: Cetacea and Microchiroptera are hypertrophied in specific

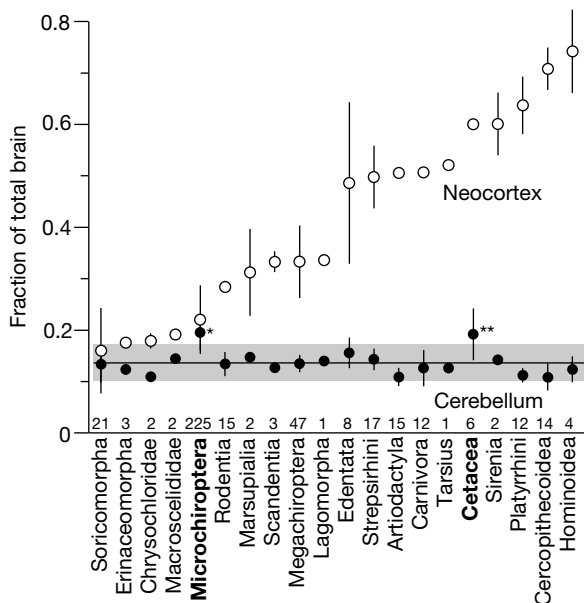


Figure 2 Constancy of cerebellar volume fraction across mammalian taxa. Cerebellar volume fractions are plotted at order level with the exception of the primates, which were divided into Strepsirhini (lemurs and lorises), Platyrrhini (New World monkeys), Cercopithecoidea (Old World monkeys) and Hominoidea (apes and human). The cerebellar volume fractions are indicated by solid symbols. Data are sorted by neocortical volume fraction (open symbols). The error bars indicate s.d.; the shaded bar indicates mean \pm 1 s.d. for the pooled data. Statistically significant differences between an individual taxon and the entire group are identified in bold (Student's t test: asterisk, $P < 0.02$; double asterisk, $P < 0.01$).

homologous parafloccular and medial regions, which in bats are responsive to acoustic target position and velocity (reviewed in ref. 14). Similarly, among teleost fishes, the largest cerebella are found in mormyrids, which electrolocate to detect object size and distance¹⁴. The common factor of echolocation and electrolocation is the interpretation of subtle timing differences in echoes returned from transmitted pulses. Thus, regardless of its overall functional role, the cerebellum seems in these species to provide additional processing power for sophisticated sensory adaptations. Our results also suggest a more general speculation: that the cerebellum provides guidance to the entire brain on the basis of fine features of sensory input.

Our observations in the whole brain led us to search for size trade-offs and constancy within the telencephalon. Normalizing to a total telencephalic volume of 1, telencephalic volume fractions T also showed high variability among orders (Fig. 1b, d). T_{neo} increased from $28 \pm 10\%$ ($n = 28$) in insectivores to $55 \pm 1\%$ ($n = 3$) in tree shrews, $81 \pm 8\%$ ($n = 44$) in primates and 95% in *Homo* (Fig. 1b, blue points). This expansion in neocortex occurred at the expense of hippocampus, septum, schizocortex, piriform cortex and olfactory bulb: the sum of these fractions decreased from $64 \pm 10\%$ in insectivores to $37 \pm 1\%$ in tree shrews, $12 \pm 7\%$ in primates and 3% in *Homo*.

In the face of this neocortical expansion, the telencephalic structure that showed the least change was the striatum (Fig. 1d, red points). The striatum maintained a volume fraction of $T_{\text{stri}} = 8 \pm 2\%$ in insectivores, $8 \pm 1\%$ in tree shrews, $6 \pm 1\%$ in primates and 3% in *Homo*. The striatum forms extensive interconnections with the hippocampus, the amygdala and nearly all of the cerebral cortex¹³. These connections form part of an extensive looped corticothalamic network that, when damaged, leads to extrapyramidal motor disorders such as Parkinson's and Huntington's disease. The relative preservation of T_{stri} is consistent with a function in motor activity that depends on the amount of telencephalic input and requires some minimum necessary amount of striatal processing.

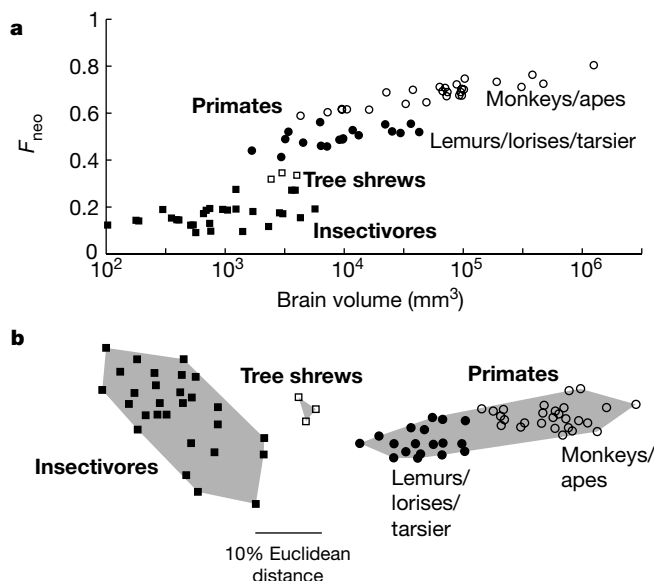


Figure 3 Clustering of cerebrotypes by taxon. **a**, Neocortical fraction of total brain volume plotted against total brain volume for insectivores (filled squares), tree shrews (open squares), lemurs, lorises and tarsier (filled circles), and monkeys and apes (open circles). **b**, Variation in the 11-component cerebrotypes for the species plotted in **a** displayed in a plane using multidimensional scaling. Compared with true Euclidean distance between cerebrotypes, the root-mean-squared (r.m.s.) fractional error in displayed interspecies distance is 8.4%.

The cerebrotypes we observe suggests that each taxon might be associated with its own distinct brain architecture. This can be seen at a coarse level by plotting a single quantity, F_{neo} , against brain volume¹. Although absolute brain volume varied several hundredfold within each order, there was little variation of F_{neo} (Fig. 3a), indicating that this fraction takes on specific values for major taxonomic divisions³.

To facilitate the identification of finer taxonomic distinctions, we used all total-brain and telencephalic volume fractions to generate a relational map of mammalian brain architectures. We did this using multidimensional scaling, an algorithm that shows the variation of all 11 volume fractions in a plane with maximum fidelity to the true distances between cerebrotypes. This method allows species to be compared without making *a priori* assumptions about allometric scaling relationships between components. Figure 3b shows clear separation between insectivores and primates. Scandentia, once categorized as primates⁶, were nearer to insectivores than to primates in cerebrotypes, but there was no overlap between either group. This assessment agrees with recent morphological and molecular evidence, and supports the identification of Scandentia as a separate mammalian lineage.

The eight 'insectivore'¹⁵ orders represented in this data set also appeared as distinct groups of points (Fig. 4a), with the exception of the overlapping cerebrotypes distributions of Soricidae (shrews) and Tenrecidae (tenrecs). This overlap arose entirely from the cerebrotypes of three tenrecs that live and/or hunt in the water (Fig. 4a). This difference from other tenrecs suggests that these three species

have brain specializations that reflect an aquatic lifestyle, such as reductions in the size of the olfactory bulbs and piriform cortex (see Supplementary Information). Thus, cerebrotypes analysis provides a means of taxonomically grouping mammals by their brain structure. The existence of these characteristic within-taxon cerebrotypes across large variations in absolute brain size suggests that brain components are scalable; that is, a functionally optimized brain has the same proportions independent of absolute volume. Furthermore, the fact that 11-component cerebrotypes can be mapped into a two-dimensional plane but still accurately represent distance information suggests that the range of possible brain architectures is strongly constrained.

Cerebrotypes-based measures might also be useful in finding directional changes in brain architecture. According to the social intelligence hypothesis of primate brain evolution⁴, a larger neocortex may confer selection advantages owing to increased cognitive capacity for use in social dynamics. This would lead to progressive, relative enlargement of the neocortex over time. Fossil and molecular evidence and morphological evidence from non-brain characters shows that successively more derived primate taxa have arisen over time: lemurs/orises, followed by tarsiers, New World monkeys, Old World monkeys, and then hominoids¹⁶. The arrangement of the corresponding cerebrotypes (Fig. 4b) is collinear with this order of primate taxa, with the exception of some overlap between New World and Old World monkeys. This overlap arises from the four New World monkeys in this database—*Ateles geoffroyi*, *Lagothrix lagotrichya*, *Cebus* sp. and *Saimiri sciureus*—with larger group sizes and complex social structures resembling those of Old World monkeys¹⁷. The cerebrotypes of New World monkeys with large group sizes differ from other New World monkeys principally in F_{neo} (large group size $69.3 \pm 0.5\%$, 4 species; other $61.8 \pm 1.7\%$, 8 species; $P < 0.001$) but are similar to Old World monkeys ($70.4 \pm 2.4\%$, 11 species; $P = 0.1$; see Supplementary Information). Taken together, these orderings suggest that increased derivation was indeed accompanied by progressive changes in the cerebrotypes, perhaps relating to social intelligence.

Cerebrotypes shifts in primates are accompanied by significant expansion of the neocortical volume fraction¹ (Fig. 3a). To identify other, independent changes in architecture, we eliminated neocortex from the data set and renormalized the remaining ten regions. Multidimensional scaling still showed clear separation of primate taxa (Fig. 4c). We obtained similar results when we also removed the cerebellum from the data set (not shown). Thus, the rise of new primate taxa has been accompanied by substantial shifts in brain architecture, marked both by increases in relative neocortical size and by distinct changes in the distribution of brain volume among other regions.

Because cerebrotypes shifts are progressive, cerebrotypes differences should be largest between groups with the oldest last common ancestor. We emphasized changes in forebrain structures by considering the telencephalic cerebrotypes. At principal points of divergence for which dates have been estimated multiple times from DNA and fossil evidence¹⁶ (Fig. 5a), the Euclidean cerebrotypes distance was calculated between groups of species on either side of each node (see Methods) (Fig. 5b). The most recent divergence points were consistently associated with shorter distances between cerebrotypes (Spearman's rank correlation coefficient $r_s = 1.00$, $P < 0.01$). By contrast, a previous metric of body-size-scaled indices³ has suggested homology between the brains of humans and spider monkeys, a result irreconcilable with known phylogeny. Therefore, among quantitative brain parameters examined to date, only the cerebrotypes provides a measure of architecture that correlates with date of divergence of advanced primates.

To test if changes in brain architecture tracked primate evolution within each major group, the method of independent contrasts (see Methods)¹⁸ was used to make comparisons among groups of species (Fig. 5c). Overall, longer cerebrotypes distances were associated

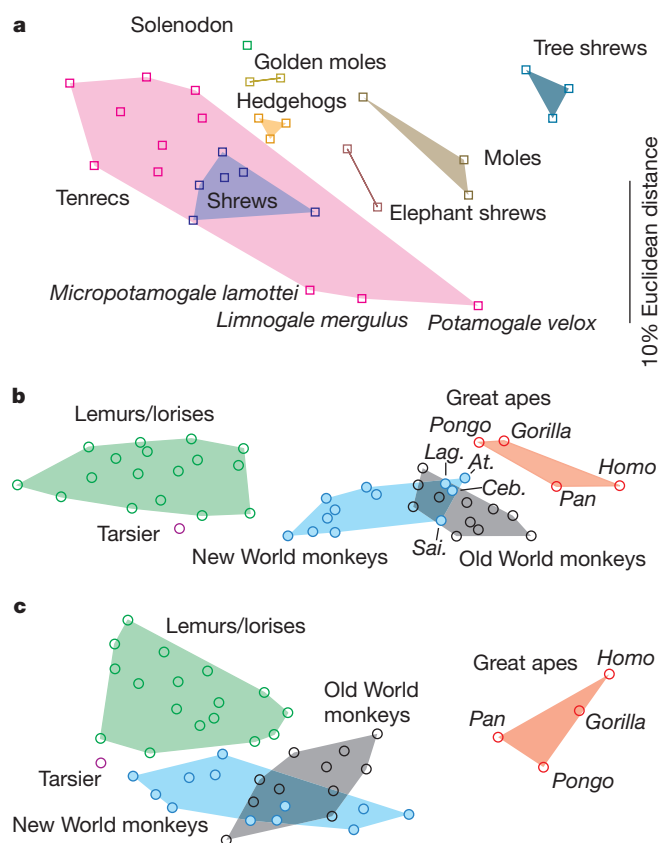


Figure 4 Clustering of cerebrotypes within taxa. **a**, Sorting of insectivore and tree shrew taxa using multidimensional scaling. Each shaded area indicates the minimum convex polygon for that taxon. The r.m.s. fractional error is 16.9%. **b**, Multidimensional scaling of primates. The r.m.s. fractional error is 6.3%. The labels for New World monkeys with complex social groupings indicate *A. geoffroyi* (At.), *L. lagotricha* (Lag.), *Cebus* sp. (Ceb.) and *S. sciureus* (Sai). **c**, Multidimensional scaling of primates on cerebrotypes data in which neocortex was excluded and the remaining ten volume fractions renormalized. The r.m.s. fractional error is 14.2%. The scale bar in **a** also refers to **b** and **c**.

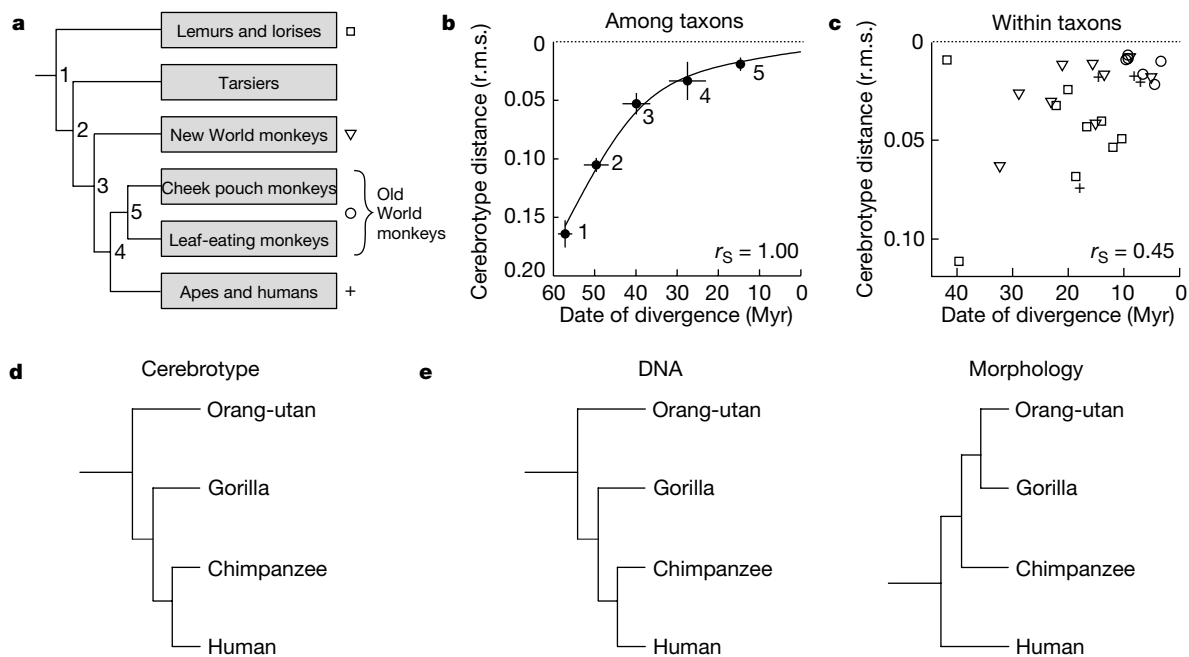


Figure 5 Evolutionary trends in brain architecture. **a**, Known phylogenetic relationships among primate taxa¹⁶ showing major divergence points (1–5). **b**, Telencephalic cerebrotypic distance between groups on either side of divergence points that are well-dated with fossil and DNA evidence. Vertical error bars indicate standard error of the mean; horizontal error bars are from ref. 16. The solid curve is a spline fit. **c**, Telencephalic

cerebrotypic distance within each taxon. Different symbols represent independent contrasts¹⁸ made within different taxa, as indicated in **a**. **d**, Relationships among hominoids reconstructed using telencephalic structures. **e**, Trees derived from DNA sequence (centre) and bone and tooth structure¹⁹ (right). The branch lengths are arbitrary.

with older divergence dates (Spearman's rank correlation coefficient $r_s = 0.45$, $P < 0.01$, $n = 28$ independent comparisons). This strong correlation led us to use distances between individual species to reconstruct the taxonomy of four hominoids (Fig. 5d). The resulting tree was identical to that obtained from DNA sequence (Fig. 5e, left), (*(Homo, Pan), Gorilla, Pongo*), but not to a tree obtained from bone and tooth morphology (Fig. 5e, right), (*Homo, (Pan, (Pongo, Gorilla))*). This lends support to the suggestion that soft tissues represent a more accurate route than hard tissues to phylogenetic reconstruction¹⁹.

Our results suggest a model for primate brain evolution in which adaptive radiation within a taxon has generated changes in the absolute brain (and also body) size while preserving an approximately fixed cerebrotypic. Shifts in cerebrotypic occurred at infrequent (about 10 Myr) intervals coinciding with the rise of new taxa. These shifts were marked primarily by relative expansion of the telencephalon, especially the neocortex. This expansion has reached an extreme in *Homo*, which possesses the largest F_{neo} value known (0.80).

Our observations suggest a reconciliation of developmentalist² and adaptationist³ models of how brain architecture is determined. Within each taxon, brain regions are scalable, tending to maintain fixed proportionality of size to one another independent of absolute total brain volume. This suggests that, within a taxon, the development of multiple brain regions is governed by a common set of mechanisms². However, because the cerebrotypic varies from taxon to taxon, these developmental mechanisms must also be variable. This variation arises from genetic modification that leads to the appearance of new cerebrotypes. For instance, in primates, the enlargement of the neocortex may be caused by the action of additional rounds of cortical neurogenesis^{20,21}. In addition to these major shifts, variations in developmental rates in other brain regions can lead to limited adaptive radiation of the cerebrotypic within each taxon. These variations may be driven by ecological and/or social requirements³. Finally, the microscopic

composition of neural tissue (neurons, glia, axons and dendrites) varies across mammals²². An ultimate explanation of these changes in brain structure will, therefore, require a deeper understanding of both the causes for variation at a cellular level and the selective advantages provided by a changing brain architecture. □

Methods

For cerebrotypic analysis, data were taken from ref. 6, consisting of 28 insectivores¹⁵, 3 Scandentia (tree shrews), 18 strepsirhine (lemur and loris) primates and 27 haplorhine (tarsier, New World and Old World monkey, and hominoid) primates. Definitions of primate species conformed to ref. 16 and definitions of brain regions conformed to ref. 6. Brain volumes ranged over four orders of magnitude. The volume fraction was defined for the five principal brain components and for the seven telencephalic components. Whole-brain volume fractions (F) were calculated for medulla oblongata, cerebellum, mesencephalon, diencephalon and telencephalon by dividing by total brain volume. Volume fractions were calculated for olfactory bulb, piriform cortex, septum, striatum, schizocortex, hippocampus and neocortex by dividing by either the whole-brain volume (fractions F) or by the telencephalic volume (fractions T). We excluded the accessory olfactory bulb, which is not present in many primates, from the analysis. We also excluded one haplorhine (*Callicebus moloch*) from the analysis because the components failed to sum to the whole in the original data. Additional data used to compare neocortical and cerebellar volume fractions across taxa (Fig. 2) were obtained from the literature for Artiodactyla^{23,24}, Carnivora²⁴, Cetacea⁹⁻¹², Edentata²⁵, Lagomorpha²⁴, Marsupialia²⁴, Microchiroptera and Megachiroptera¹³, Rodentia^{26,27}, Sirenia^{28,29}, and orang-utan³⁰. All values are given as mean \pm s.d. unless otherwise noted.

Independent contrasts

We arranged species in a tree according to a published primate phylogeny¹⁶. At each node, two mean cerebrotypes were calculated, one for each branch emanating from the node. The Euclidean distance between the two means was used to make a comparison for that node, the method of independent contrasts¹⁸.

Phylogenetic reconstruction

The telencephalic cerebrotypic was defined as T , the vector of telencephalic volume fractions. For hominoids, a phylogenetic tree was constructed from cerebrotypic distances using the Fitch–Margoliash algorithm, which sequentially adds species to a test tree while minimizing the quantity $\sum \Sigma (o_{ij} - e_{ij})^2 / o_{ij}^2$, where o_{ij} is the Euclidean cerebrotypic distance between species i and j , and e_{ij} is the total length of the path joining the two species in the test tree. Colobinae (leaf-eating monkeys) were used as the outgroup to root the tree. Optimization and display were done using the PHYLIP software package running on a PC-DOS platform.

Multidimensional scaling

Multidimensional scaling was done using MATLAB (The Mathworks, Natick, MA) to allow simultaneous display of variation in all 11 *F* components (principal brain divisions and telencephalic components) of the cerebrotypes. The quantity $\sum(o_{ij} - d_{ij})^2 / o_{ij}^2$ was minimized where o_{ij} is the cerebrotypes distance and d_{ij} is the displayed distance in the plane. Minimizations were done using a bootstrapping procedure. The plot was initially seeded using three points chosen by a trial run to lie near the outskirts of the final plot. We added subsequent points one at a time in a random order. After each point was added, a round of error minimization was performed in which only the new point was allowed to vary, followed by a round of minimization in which all points were varied. Each minimization was performed at least ten times and the solution with the least error was accepted. In the 76-point minimization of all species (Fig. 3b), new points were added four at a time. This overall procedure resembles the Fitch–Margoliash algorithm for phylogeny reconstruction but yields a mapping in a plane rather than a connected tree.

Received 28 November 2000; accepted 12 March 2001.

1. Jerison, H. J. *Brain Size and the Evolution of Mind* (American Museum of Natural History, New York, 1991).
2. Finlay, B. L. & Darlington, R. B. Linked regularities in the development and evolution of mammalian brains. *Science* **268**, 1578–1584 (1995).
3. Barton, R. A. & Harvey, P. H. Mosaic evolution of brain structure in mammals. *Nature* **405**, 1055–1058 (2000).
4. Barton, R. A. & Dunbar, R. I. M. in *Machiavellian Intelligence II* (eds Whiten, A. W. & Byrne, R. W.) 240–263 (Cambridge Univ. Press, New York, 1992).
5. Douglas, R. J. & Marcellus, D. The ascent of man: deductions based on a multivariate analysis of the brain. *Brain Behav. Evol.* **11**, 179–213 (1975).
6. Stephan, H., Frahm, H. & Baron, G. New and revised data on volumes of brain structures in insectivores and primates. *Folia Primatol.* **35**, 1–29 (1981).
7. Aiello, L. C. & Wheeler, P. The expensive-tissue hypothesis: the brain and digestive system in primate evolution. *Curr. Anthropol.* **36**, 199–221 (1995).
8. Airapet'yants, E. S. & Konstantinov, A. I. *Echolocation in Animals* (Keter, Jerusalem, 1973).
9. Jansen, J. On the whale brain with special reference to the weight of the fin whale (*Balaenoptera physalus*). *Norsk Hvalfangst-tidende* **9**, 480–486 (1952).
10. Pilleri, G. Morphologie des ghirnes des "Southern Right Whale". *Acta Zool.* **46**, 245–272 (1964).
11. Jansen, J. & Jansen, J. K. S. in *The Biology of Marine Mammals* (ed. Andersen, H. T.) 175–252 (Academic, New York, 1969).
12. Ridgway, S. H. in *The Bottlenosed Dolphin, Tursiops spp.* (eds Leatherwood, J. S. & Reeves, R.) 69–97 (Academic, San Diego, 1989).
13. Baron, G., Stephan, H. & Frahm, H. D. *Comparative Neurobiology in Chiroptera: Macromorphology, Brain Structures, Tables, and Atlases* (Birkhauser, Basel, 1996).
14. Paulin, M. G. The role of the cerebellum in motor control and perception. *Brain Behav. Evol.* **41**, 39–50 (1993).
15. Mouchaty, S. K., Gullberg, A., Janke, A. & Arnason, U. The phylogenetic position of the Talpidae within Eutheria based on analysis of complete mitochondrial proteins. *Mol. Biol. Evol.* **17**, 60–67 (2000).
16. Purvis, A. A composite estimate of primate phylogeny. *Phil. Trans. R. Soc. Lond. B* **348**, 405–421 (1995).
17. Kinzey, W. G. *New World Primates: Ecology, Evolution, and Behavior* (Aldine de Gruyter, New York, 1997).
18. Harvey, P. H. & Pagel, M. *The Comparative Method in Evolutionary Biology* (Oxford Univ. Press, Oxford, 1991).
19. Gura, T. Bones, molecules...or both? *Nature* **406**, 230–233 (2000).
20. Xuan, S. *et al.* Winged helix transcription factor BF-1 is essential for the development of the cerebral hemispheres. *Neuron* **14**, 1141–1152 (1995).
21. Kornack, D. R. & Rakic, P. Changes in cell-cycle kinetics during the development and evolution of primate neocortex. *Proc. Natl Acad. Sci. USA* **95**, 1242–1246 (1998).
22. Braitenberg, V. & Schüz, A. *Cortex: Statistics and Geometry of Neuronal Connectivity* (Springer, Berlin, 1998).
23. Kruska, D. & Rohrs, M. Comparative-quantitative investigations on brains of feral pigs from the Galapagos Islands and of European domestic pigs. *Z. Anat. Entwicklungsgesch* **144**, 61–73 (1974).
24. Meyer, J. A quantitative comparison of the parts of the brains of two Australian marsupials and some eutherian mammals. *Brain Behav. Evol.* **18**, 60–71 (1981).
25. Pirlot, P. & Kamiya, T. Quantitative brain organization in anteaters (Edentata-Tubilidentata). *J. Hirnforsch.* **24**, 677–689 (1983).
26. Fox, J. H. & Wilczynski, W. Allometry of major CNS divisions: towards a reevaluation of somatic brain–body scaling. *Brain Behav. Evol.* **28**, 157–169 (1986).
27. Frahm, H. D., Rehkämper, G. & Nevo, E. Brain structure volumes in the mole rat, *Spalax ehrenbergi* (Spalacidae, Rodentia) in comparison to the rat and subterranean insectivores. *J. Brain Res.* **38**, 209–222 (1997).
28. Reep, R. L. & O'Shea, T. J. Regional brain morphometry and lissencephaly in the Sirenia. *Brain Behav. Evol.* **35**, 185–194 (1990).
29. Pirlot, P. & Kamiya, T. Qualitative and quantitative brain morphology in the Sirenia Dugong dugong Erxl. *Z. Zool. Syst. Evol.-forsch.* **23**, 147–155 (1985).
30. Zilles, K. & Rehkämper, G. in *Orang-utan Biology* (ed. Schwartz, J. H.) 157–176 (Oxford Univ. Press, New York, 1988).

Supplementary information is available on Nature's World-Wide Web site (<http://www.nature.com>) or as paper copy from the London editorial office of Nature.

Acknowledgements

We thank J. M. Allman and M. J. Berry for discussions, R. Kasthuri for research assistance, and T. A. Barney for secretarial assistance. D.A.C. is in the Princeton University Program in Biophysics. S.S.-H.W. is supported by the Alfred P. Sloan Foundation.

Correspondence and requests for materials should be addressed to S.S.-H.W. (e-mail: samwang@molbio.princeton.edu).

An evolutionary scaling law for the primate visual system and its basis in cortical function

Charles F. Stevens

The Salk Institute and Howard Hughes Medical Institute, 10010 North Torrey Pines Road, La Jolla, California 92037, USA

A hallmark of mammalian brain evolution is the disproportionate increase in neocortical size as compared with subcortical structures¹. Because primary visual cortex (V1) is the most thoroughly understood cortical region, the visual system provides an excellent model in which to investigate the evolutionary expansion of neocortex. I have compared the numbers of neurons in the visual thalamus (lateral geniculate nucleus; LGN) and area V1 across primate species. Here I find that the number of V1 neurons increases as the 3/2 power of the number of LGN neurons. As a consequence of this scaling law, the human, for example, uses four times as many V1 neurons per LGN neuron (356) to process visual information as does a tarsier (87). I argue that the 3/2 power relationship is a natural consequence of the organization of V1, together with the requirement that spatial resolution in V1 should parallel the maximum resolution provided by the LGN. The additional observation that thalamus/neocortex follows the same evolutionary scaling law as LGN/V1 may suggest that neocortex generally conforms to the same organizational principle as V1.

Any study of evolutionary scaling relations—the allometric laws that relate the size of one structure to another—must deal with species that are homogeneous in their scaling properties. Various taxonomic orders or suborders can conform to scaling laws with the same power but different scale factors². The data presented here are for haplorhine primates, a suborder that appears to be homogeneous with respect to the brain areas that I consider.

Figure 1 plots the number of neurons in V1 as a function of number of LGN neurons for 23 haplorhines whose average brain volumes range from 3.4 cm³ (tarsier) to 1,252 cm³ (human). This figure is derived from data presented by various authors as indicated in the Methods. A nonlinear fit reveals that these data are well described by a power law with an exponent of 3/2 (1.54 ± 0.07). That is, across the haplorhines the number of V1 neurons *N* varies

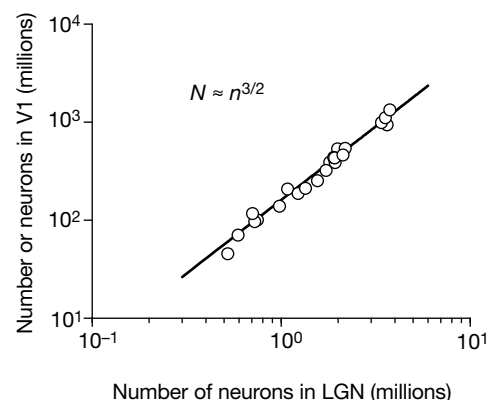


Figure 1 Number of neurons in V1 (*N*) as a function of number of LGN neurons (*n*) for 23 haplorhine primates. The smooth lines are power functions with exponents of 3/2 and 1.54 (the best fit to the data). For this graph, the tarsier has the smallest LGN/V1 ratio, and the human the largest.